ESR Fine Structure of Manganese Ions in Zeolite A Detects Strong Variations of the Coordination Environment

Dirk E. De Vos,[†] Bert M. Weckhuysen,[‡] and Thomas Bein*,[†]

Contribution from the Department of Chemistry, Purdue University, West Lafayette, Indiana 47907, and Centrum voor Oppervlaktechemie en Katalyse, K. U. Leuven, Kardinaal Mercierlaan 92, 3001 Heverlee, Belgium

Received January 2, 1996[⊗]

Abstract: The electron spin resonance spectra of Mn^{2+} exchanged zeolite A have been investigated as a function of the monovalent co-cation (K^+, Na^+, Li^+, Cs^+, or NH_4^+), Mn^{2+} content, recording frequency, and temperature. Three new Mn^{2+} species are observed with a well-resolved fine structure; this allows for the first time a direct quantitative determination of the zero-field splitting (ZFS) parameters in zeolites. In hydrated zeolites, three ESR active Mn^{2+} species are observed, characterized by different values for the ZFS parameter D. Species **I** has $D = 0.035$ cm^{-1}. Species **II** is closer to a regular octahedron, with $D = 0.010$ cm^{-1}. Species **III**, with $D = 0.14$ cm^{-1}, is in a strongly axially distorted coordination. Species **I** is dominant in MnKA, MnCsA, and $MnNH_4A$, while **II** and **III** are found in MnNaA and MnLiA. In fully dehydrated zeolites, two species are observed. Species **IV** has a small hyperfine constant A and is present in dry NaA and KA. Species **V** is observed in dry LiA; it has axial symmetry with a large, temperature-dependent D. Species **V** probably represents Mn^{2+} in a 3-fold coordination in a 6-ring. In partially hydrated zeolites, a tetrahedral species **VI** is observed. The spectroscopic data elucidate the location of manganese(II) ions in zeolite A, particularly at relatively low metal loadings.

Introduction

The ESR fine structure of transition metal ions with several unpaired electrons, such as high-spin Mn^{2+}, Fe^{3+}, and Cr^{3+}, is determined by the splitting of the energy levels in zero field. Analysis of the zero-field splitting (ZFS) parameters D and E provides direct insight into the symmetry and coordination of these ions. Especially for Mn^{2+}, where common techniques such as electronic spectroscopy and magnetic measurements yield little useful information, the analysis of the ZFS parameters based on the ESR spectra has been extremely helpful in elucidating the structure of numerous Mn^{2+} compounds.[1]

In the study of the coordination and siting of transition metal ions in zeolites and related molecular sieves, ESR has been a major tool.[2] However, most studies have concentrated on intrazeolitic d^1 or d^9 metal ions, where structural information is obtained primarily from anisotropy in the $\boldsymbol{g}$ or $\boldsymbol{A}$ tensor. For ions with higher spin multiplicity, knowledge of the ZFS parameters is essential for structural understanding. However, in the case of Fe^{3+} and Cr^{3+}, the typical zeolite spectra do not display sufficient resolution for quantitative determination of D and E.[3,4] In a recent detailed study, Goldfarb *et al.* discuss the role of ZFS in the spectrum of iron-containing zeolites.[4] One usually observes the limiting situations $g_{\text{eff}} = 2$ (cubic symmetry, D and $E \ll h\nu$) and $g_{\text{eff}} = 4.3$ (rhombic symmetry, $D \gg h\nu$, E/D close to 1/3).

In the specific case of Mn^{2+} molecular sieves, earlier ESR studies have mainly been concerned with X or Y zeolites.[5,6] Variations of the co-cation population and hydration of these zeolites influence the ESR spectra, and at least five different Mn^{2+} species have been proposed in Y zeolites alone. In addition, the spectra of Mn-substituted (silico)aluminophosphate or mesoporous molecular sieves have been reported and discussed.[7] A common characteristic of all reported spectra of Mn^{2+} in molecular sieves is that only the central $M_S = +1/2 \leftrightarrow -1/2$ transition is resolved; the non-central fine lines are typically broadened, making it difficult to determine D and E. Nevertheless, knowledge of the ZFS parameters is important, as any departure from a cubic octahedral or tetrahedral symmetry is expressed primarily by changes of the ZFS parameters.

In this work, we report for the first time on the direct observation of the fine structure in the ESR spectra of Mn^{2+}-exchanged A zeolites. The X- and Q-band ESR spectra of Mn^{2+} in this zeolite are strongly influenced by the nature of the co-cation (Li^+, Na^+, K^+, Cs^+, and NH_4^+) and by the hydration state of the molecular sieve. Attention is directed primarily toward the identification of the spectral features. Apart from three Mn^{2+} species with small ZFS, previously reported for zeolite A, we describe three new Mn^{2+} species with well-observable fine-splitting patterns. From these, reliable values for the fine-splitting parameter D are derived. These data are

* Author to whom correspondence should be addressed.
† Purdue University.
‡ Centrum voor Oppervlaktechemie en Katalyse.
⊗ Abstract published in *Advance ACS Abstracts,* August 1, 1996.

(1) (a) Dowsing, R. D.; Gibson, J. F.; Goodgame, D. M. L.; Goodgame, M.; Hayward, P. J. *Nature* **1968**, *219*, 1037. (b) Goodgame, M.; Okey, J. N. *J. Chem. Soc., Dalton Trans.* **1985**, 75.

(2) (a) Kevan, L. *Acc. Chem. Res.* **1987**, *20*, 1. (b) Kevan, L. *Electron Spin Resonance, A Specialist Periodical Report* **1991**, *12B*, 99. (c) Schoonheydt, R. A. *Catal. Rev. Sci. Eng.* **1993**, *35*, 129.

(3) Pearce, J. R.; Sherwood, D. E.; Hall, M. B.; Lunsford, J. H. *J. Phys. Chem.* **1980**, *84*, 3215.

(4) Goldfarb, D.; Bernardo, M.; Strohmaier, K. G.; Vaughan, D. E. W.; Thomann, H. *J. Am. Chem. Soc.* **1994**, *116*, 6344.

(5) (a) Barry, T. I.; Lay, L. A. *Nature* **1965**, *208*, 1312. (b) Barry, T. I.; Lay, L. A. *J. Phys. Chem. Solids* **1966**, *27*, 1821. (c) Barry, T. I.; Lay, L. A. *J. Phys. Chem. Solids* **1968**, *29*, 1395.

(6) (a) Tikhomirova, N. N.; Nikolaeva, I. V.; Demkin, V. V.; Rosolovskaya, E. N.; Topchieva, K. V. *J. Catal.* **1973**, *29*, 105. (b) Tikhomirova, N. N.; Nikolaeva, I. V.; Demkin, V. V.; Rosolovskaya, E. N.; Topchieva, K. V. *J. Catal.* **1973**, *29*, 500. (c) Tikhomirova, N. N.; Nikolaeva, I. V.; Rosolovskaya, E. N., Demkin, V. V.; Topchieva, K. V. *J. Catal.* **1975**, *40*, 61. (d) Tikhomirova, N. N.; Nikolaeva, I. V. *J. Catal.* **1975**, *40*, 135. (e) Tikhomirova, N. N.; Nikolaeva, I. V. *Zh. Fiz. Khim.* **1981**, *55*, 2224.

(7) (a) Lee, C. W.; Chen, X.; Brouet, G.; Kevan, L. *J. Phys. Chem.* **1992**, *96*, 3110. (b) Brouet, G.; Chen, X.; Lee, C. W.; Kevan, L. *J. Am. Chem. Soc.* **1992**, *114*, 3720. (c) Levi, Z.; Raitsimring, A. M.; Goldfarb, D. *J. Phys. Chem.* **1991**, *95*, 7830. (d) Zhao, D.; Goldfarb, D. *J. Chem. Soc., Chem. Commun.* **1995**, 875.

S0002-7863(96)00012-1 CCC: $12.00

compared to spectroscopic data for other cations, and the implications for the distribution of Mn^{2+} over different cation sites in zeolite A are discussed.

Experimental Section

KA (from Alfa) and NaA zeolites (from PQ) were used in this work. LiA was obtained by stirring NaA three times in a 5-fold LiCl excess at 333 K for 6 h, followed by extensive washing with deionized water. An analogous procedure, using a 3-fold excess of CsCl or NH_4Cl, was applied to obtain CsNaA, CsKA, and NH_4A zeolites. Mn^{2+} exchanges were performed for a minimum of 3 h at room temperature, by stirring the hydrated zeolite in dilute solutions of $MnCl_2 \cdot 4H_2O$ (Mallinckrodt). A minimum volume to zeolite weight ratio of 100 mL per g and a maximum Mn concentration of 2 mM were used. The pH during exchange was kept between 6 and 7 by addition of dilute HCl to prevent the base-promoted oxidation of Mn^{2+} to Mn^{3+}.[8] The resulting white suspensions were filtered and washed with copious amounts of deionized water. A high crystallinity of the Mn^{2+}-exchanged zeolites was confirmed by X-ray diffraction using a XDS 2000 diffractometer of Scintag. The Mn contents were 0.025, 0.1, 0.4, 1.7, and 10.0 wt %. Zeolites were dehydrated by heating under a flow of oxygen at a rate of 1 K per min up to 673 K; this temperature was maintained for 6 h. Rehydration was performed by exposure of the dehydrated zeolites at room temperature to a relative humidity of 79% over a saturated NH_4-Cl solution.

X-band ESR spectra of the Mn zeolite samples were recorded with a Bruker ESP-300 apparatus between 7 and 400 K. Q-band ESR spectra were obtained with a Varian spectrometer with cooling accessory. ESR spectral simulations were performed with the Q-Pow simulation program of Dr. M. Nilges (University of Illinois at Urbana−Champaign). Magnetic susceptibility measurements were performed using a MPMS SQUID magnetometer in a field of 0.1 T.

Results

Samples with a Mn^{2+} content between 0.025 and 0.4 wt % have ESR spectra with optimum signal-to-noise ratios, whereas higher Mn loadings resulted in a serious loss of spectral resolution, presumably due to dipolar interactions. At 10 wt % Mn, there is only one, structureless absorption.

ESR fine-splitting patterns may arise not only from monomeric species but also from species with more nuclei; for example, fine structure is well documented for Mn−Mn pairs in CaO, or for Cu−Cu pairs in some Y zeolites.[9] In the absence of hyperfine structure, occurrence of Mn pairs or larger aggregates may thus be difficult to exclude. Therefore MnKA, MnLiA, and MnNaA (0.4 wt % Mn) were subjected to SQUID magnetization measurements at constant field (0.1 T) between 10 and 200 K. In this temperature range, the Mn in these zeolites displayed essentially identical Curie behavior, even if the ESR spectra varied considerably. Therefore it seems that fine structure in the ESR spectra is due to different coordination geometries of mononuclear Mn species, rather than to the presence of Mn aggregates.

The line identification for Mn^{2+} ESR powder spectra is based on the evaluation of the spin Hamiltonian developed by Abragam and Bleaney.[10] In the case of axial symmetry, the zero-field splitting is described by the parameter D. For Mn^{2+}, with $S = {}^5/_2$, this results in a splitting of the resonance into five fine transitions ($M_S = +{}^1/_2 \leftrightarrow -{}^1/_2$; $M_S = \pm{}^3/_2 \leftrightarrow \pm{}^1/_2$; $M_S = \pm{}^5/_2 \leftrightarrow \pm{}^3/_2$). In powder spectra, the position of these lines is a function of θ, the angle between the local axis of symmetry and the external magnetic field. The most intense lines in the spectrum correspond to the $\theta = 90°$ maxima of the five $\Delta M_S = \pm 1$ transitions, which are separated in first order by D.[11] The absorption at other angles tends to be weak, with the exception of the $\theta = 41.8°$ orientation, where the central $M_S = +{}^1/_2 \leftrightarrow -{}^1/_2$ transition has another intensity maximum. Each of these six lines is further split into a sextet by the interaction with the Mn nuclear spin $I = {}^5/_2$. Apart from these allowed $\Delta M_S = \pm 1$, $\Delta M_I = 0$ lines, forbidden $\Delta M_S = \pm 1$, $\Delta M_I = \pm 1$ transitions are often observed, and they gain intensity at lower measurement frequency.[10b] Typically, they give rise to five doublets between the six hyperfine components of the allowed $M_S = \pm{}^1/_2 \leftrightarrow -{}^1/_2$ transition. Finally, around half field, the forbidden $\Delta M_S = \pm 2$ transitions may be observed.

Several criteria can be used to determine the magnitude of D from powder spectra. The most obvious method consists in the evaluation of the positions of the $\theta = 90°$ absorption maxima of the allowed $\Delta M_S = \pm 1$, $\Delta M_I = 0$ transitions, which are roughly spaced by D. However, due to their angle dependence, the four outer transitions may be smeared out beyond resolution. Secondly, one may use the (relative) positions of the $\theta = 90°$ and 41.8° absorption maxima of the central $M_S = +{}^1/_2 \leftrightarrow -{}^1/_2$ fine line.[12,13] These are subject to small shifts, proportional to D^2/H_0, downfield ($\theta = 90°$) or upfield ($\theta = 41.8°$) from H_0, which is the field value where resonance would occur in the absence of fine structure. Finally, the amplitudes of the forbidden $\Delta M_S = \pm 1$, $\Delta M_I = \pm 1$ lines are related to $(D/H_0)^2$, while the shifts of their positions are proportional to D^2/H_0.[14,15]

1. Hydrated MnKA Zeolites. (a) X-band Spectra. The room temperature X-band spectrum of a representative MnKA sample is given in Figure 1a. The central hyperfine sextet with $A = 0.0089 \pm 0.0001$ cm^{-1} is readily identified as the $M_S = +{}^1/_2 \leftrightarrow -{}^1/_2$ transition ($\theta = 90°$) of the Mn^{2+} ion. The two broad lines at lower field and the group of lines upfield of this $M_S = +{}^1/_2 \leftrightarrow -{}^1/_2$ sextet display only limited hyperfine structure at 298 K. Cooling of the sample to 7 K left the overall spectral features unaltered. This confirms that the spectrum originates from a monomeric Mn^{2+} species.[16] An observation at 333 K, however, reveals a better resolved hyperfine structure (Figure 1b). The shape of the line pattern at 333 K suggests the presence of Mn^{2+} in an axially distorted environment. By numerical simulation of a corresponding powder pattern, stick spectra were generated for the positions of the fine and hyperfine structure lines and these are included in Figure 1b. Four of the five $\theta = 90°$ fine lines, with 6-fold hyperfine splitting, are easily identified and were labeled as **1**, **2**, **3**, and **5**. The lack of resolution around 3800 G, where the fifth sextet is expected, is due to the overlap between the remaining $\theta = 90°$ sextet, labeled as **4**, and the $\theta = 41.8°$ absorption maximum of the $M_S = +{}^1/_2 \leftrightarrow -{}^1/_2$ transition, labeled as **3′**. From such simulations, D was estimated to amount to 0.035 ± 0.002 cm^{-1}. Note that the central $\theta = 90°$ sextet is centered around a $g_{\text{eff}} = 2.052$. Compared to hydrated Mn^{2+} in faujasites, this represents a downfield shift of about 80 G, in agreement with the calculated shift ($-2D^2/H_0$).[11] This axially distorted Mn^{2+} species in the KA zeolite is labeled as species **I**.

(8) Baes, C. F.; Mesmer, R. E. *The Hydrolysis of Cations*; Wiley: New York, 1976; p 220.
(9) (a) Harris, E. A. *J. Phys. C: Solid State Phys.* **1972**, *5*, 338. (b) Chao, C. C.; Lunsford, J. H. *J. Chem. Phys.* **1972**, *57*, 2890.
(10) (a) Bleaney, B.; Ingram, D. J. E. *Proc. R. Soc. (London)* **1951**, *A205*, 336. (b) Bleaney, B.; Rubins, R. S. *Proc. Phys. Soc.* **1961**, *77*, 103; **1961**, *78*, 778 (corrigendum).
(11) Woltermann, G. M.; Wasson, J. R. *Inorg. Chem.* **1973**, *12*, 2366.
(12) Shepherd, R. A.; Graham, W. R. M. *J. Chem. Phys.* **1984**, *81*, 6080.
(13) Tikhomirova, N. N.; Dobryakov, S. N.; Nikolaeva, I. V. *Phys. Status Solidi A* **1972**, *10*, 593.
(14) De Wijn, H. W.; Van Balderen, R. F. *J. Chem. Phys.* **1967**, *46*, 1381.
(15) Shaffer, J. S.; Farach, H. A.; Poole, C. P. *Phys. Rev. B* **1976**, *13*, 1869.
(16) Khangulov, S. V.; Pessiki, P. J.; Barynin, V. V.; Ash, D.; Dismukes, G. C. *Biochemistry* **1995**, *34*, 2015.

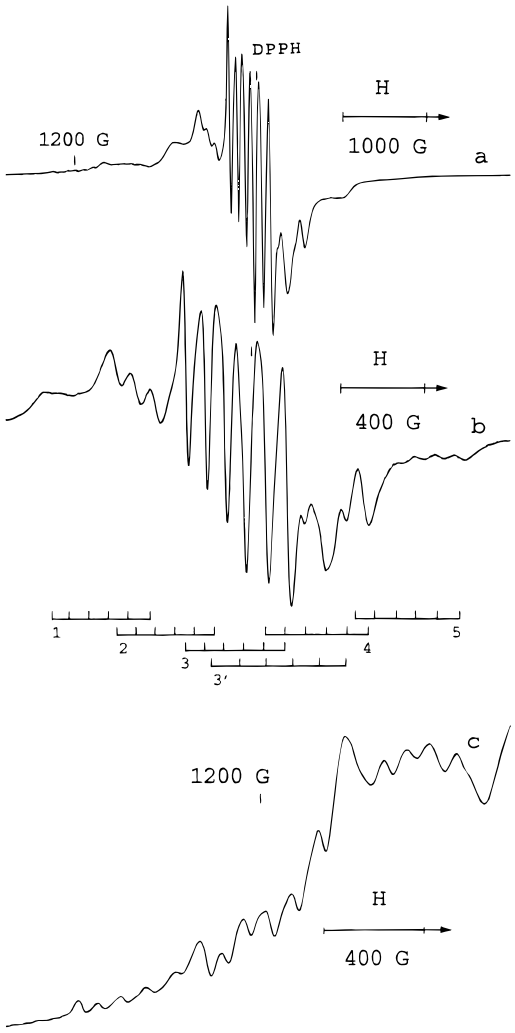

Figure 1. X-band ESR spectra of hydrated MnKA zeolite (0.1 wt % Mn): (a and c) 298 K, (b) 333 K. For the stick diagram in b, positions were calculated with $D = 0.035$ cm^{-1} and $A = 0.0089$ cm^{-1}. Labels for b are as follows: 1 and 5, $M_S = \pm^5/_2 \leftrightarrow \pm^3/_2$, $\theta = 90°$; 2 and 4, $M_S = \pm^3/_2 \leftrightarrow \pm^1/_2$, $\theta = 90°$: 3, $M_S = +^1/_2 \leftrightarrow -^1/_2$, $\theta = 90°$; 3′, $M_S = +^1/_2 \leftrightarrow -^1/_2$, $\theta = 41.8°$.

Cooling of the samples invariably resulted in a broadening of the hyperfine lines or, for the non-central fine lines, even loss of hyperfine resolution. For Mn^{2+} ions in various solvents, line broadening upon temperature decrease has been attributed to a slower Brownian rotation of the complex as a whole, or to the slower fluctuations in the coordination sphere geometry.[17] Cooling of the hydrated zeolite is expected to slow or ultimately freeze molecular motions in the proximity of the Mn sites. As a result, the fluctuations of the complex geometry become static, which leads to a distribution of the crystal-field parameters. It has been pointed out by Feher and by Dowsing and Ingram that especially the non-central lines of the fine structure are broadened by a distribution of the ZFS parameters, while the central transition is only slightly affected.[18]

Nevertheless, a clear trend can be discerned in the spectra of species **I** as the temperature is lowered. The non-central fine lines shift further away from $g = 2$. From this variation, a gradual increase of the axial zero field splitting parameter can be inferred, bringing D to 0.039 ± 0.002 cm^{-1} at temperatures below 140 K. Meanwhile, the position of the central sextet varies with T, as plotted in Figure 2. At low temperature, this sextet is centered at $g_{eff} = 2.068$, confirming the marked increase of the D parameter.

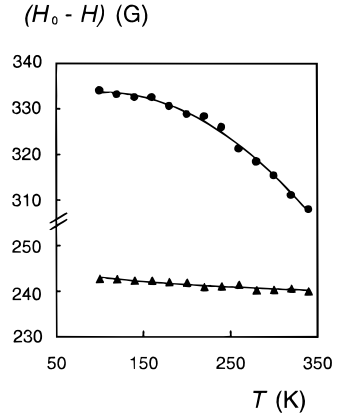

Figure 2. Temperature dependence of the position of the $\theta = 90°$ absorption maximum of the central $M_S = +^1/_2 \leftrightarrow -^1/_2$ transition of species **I** (in MnKA, ●) and species **II** (in MnNaA, ▲). Positions are expressed as downfield shifts ($H_0 - H$, G) from the DPPH resonance (H_0), and were measured at the most downfield hyperfine line of the sextet (H). For both species, $A = 0.0089$ cm^{-1} at all temperatures; hence the shifts for species **I** are due to a changing D value.

A series of low-intensity lines is observed in the low-field domain between 400 and 2200 G, where eventually the $\Delta M_S = \pm 1$, $\theta = 90°$ lines become dominant (Figure 1c). Several Mn hyperfine sextets are well resolved. Two types of lines might contribute to the absorption in this domain. First, the $\theta = 0°$ absorption edges of the $\Delta M_S = \pm 1$ transitions are spread around $g = 2$ over a range approximately twice as broad as encompassed by the $\theta = 90°$ absorption maxima. However, some of the observed sextets extend much more downfield. It is therefore probable that at least part of these lines stem from the fine and hyperfine structure of the forbidden $\Delta M_S = \pm 2$ transitions. For $D = 0.035$ cm^{-1} and at X-band, the integrated intensity of these forbidden transitions is expected to be about 4% of that of the allowed $\Delta M_S = \pm 1$ transitions.[14] However, it proved difficult to sort these lines into the expected four sextets, the zero-field splitting being relatively large in comparison with the X-band Zeeman energy.

(b) Q-band Spectra. Q-band measurements were undertaken to check the values of the splitting parameters estimated from the X-band experiments and a typical spectrum is given in Figure 3a. As the second-order shifts of the positions of the fine lines are inversely proportional to H_0, they are much smaller at Q-band frequency.[11] As a result, a highly precise simulation of the line positions could be obtained, predicting the resonance positions within 4 G, *i.e.* the error on the field determination. D was determined at 0.0356 ± 0.0004 cm^{-1} at room temperature. At high Mn concentrations, two broad shoulders are observed around the main $\theta = 90°$ absorptions (Figure 3b). These features find their origin in the $\theta = 0°$ absorption edges of the allowed $M_S = \pm 1$ transitions. As the lower field limit of these $\theta = 0°$ lines is about 10000 G, these lines are well separated at Q-band frequency from possible half-field transitions.

The ratio of the intensities of the half-field $\Delta M_S = \pm 2$ lines relative to the $\Delta M_S = \pm 1$ lines is proportional to $(D/H_0)^2$. Half-field transitions are therefore about 14 times weaker at Q-band than at X-band. At 298 and at 100 K, a broad line can be distinguished at 6300 G, which agrees well with $H_0/2$ (Figure 3c). This envelope is expected to contain four groups of lines,

(17) (a) Burlamacchi, L. *J. Chem. Phys.* **1971**, *55*, 1205. (b) Burlamacchi, L. *Gazz. Chim. Ital.* **1976**, *106*, 347. (c) Garrett, B. B.; Morgan, L. O. *J. Chem. Phys.* **1966**, *44*, 890.

(18) (a) Feher, E. R. *Phys. Rev.* **1964**, *136*, A145. (b) Dowsing, R. D.; Ingram, D. J. E. *J. Magn. Reson.* **1969**, *1*, 517.

(19) Cordischi, D.; Nelson, R. L.; Tench, A. J. *Trans. Faraday Soc.* **1969**, *65*, 2740.

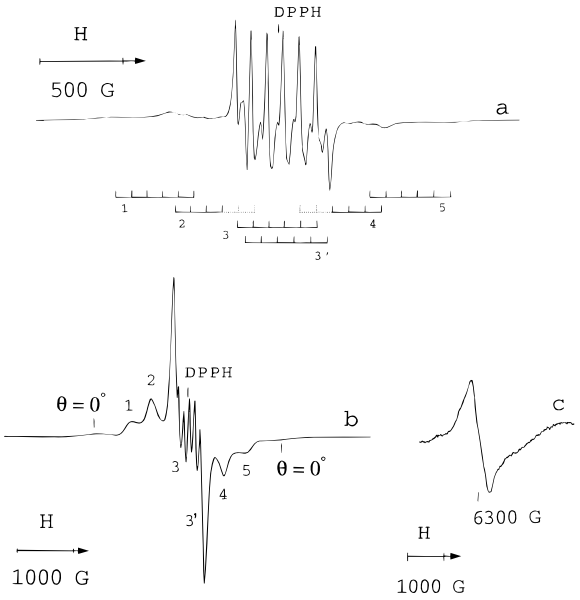

Figure 3. Q-band ESR spectra of hydrated MnKA zeolites: (a) 0.1 wt %, 298 K, (b, c) 1.7 wt %, 298 K. The positions of the stick diagram in a were calculated with $D = 0.0356$ cm^{-1} and $A = 0.0089$ cm^{-1}. Labels for a and b are as follows: 1 and 5, $M_S = \pm^5/_2 \leftrightarrow \pm^3/_2$, $\theta = 90°$; 2 and 4, $M_S = \pm^3/_2 \leftrightarrow \pm^1/_2$, $\theta = 90°$; 3, $M_S = +^1/_2 \leftrightarrow -^1/_2$, $\theta = 90°$; 3′, $M_S = +^1/_2 \leftrightarrow -^1/_2$, $\theta = 41.8°$. The markers in b indicate the $\theta = 0°$ shoulders of the $\Delta M_S = \pm 1$ transitions. Spectrum c shows the half-field transition.

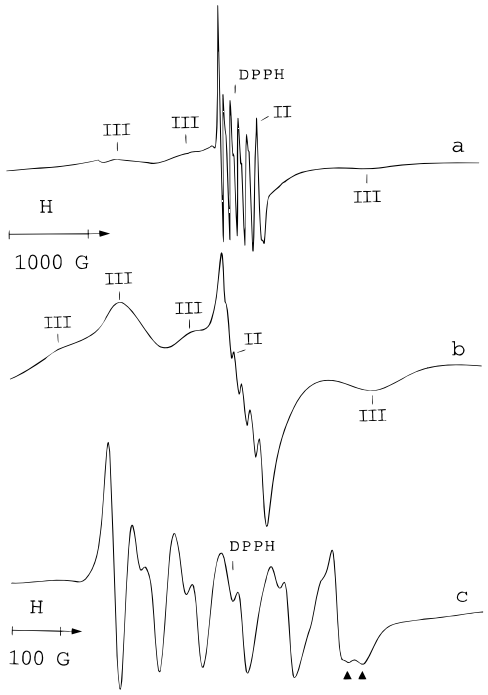

Figure 4. X-band ESR spectra of hydrated MnNaA zeolites, showing lines of species **II** and **III**: (a and c) 0.1 wt %, 298 K, (b) 1.7 wt %, 298 K. In c the ▲ symbols indicate the splitting between the $\theta = 90°$ and 41.8° sextets for $M_S = +^1/_2 \leftrightarrow -^1/_2$ in species **II**.

separated in first order by D; the two inner groups of fine lines should be twice as intense as the two outer groups.[10] This corresponds well to the overall appearance of the spectrum, with a peak-to-peak width of 540 G.

2. Hydrated MnNaA Zeolites. (a) X-band Spectra. In the spectrum of hydrated MnNaA, two groups of lines can be distinguished. First, a sextet dominates the X-band spectrum of Figure 4a. The center of this sextet with $A = 0.0089$ cm^{-1} is situated at $g_{\text{eff}} = 2.006$, which indicates that for this species, the zero-field splitting must be much smaller than for species **I**, which dominated the spectrum in the case of MnKA. We propose this Mn species **II** to be an almost octahedral Mn complex. The non-central fine transitions were not observed for this species. At the high-field end of the central sextet, a small splitting, between 25 and 35 G, is visible (Figure 4c). It is reasonable to assume that these two lines belong to the $\theta = 90°$ and 41.8° sextets. Following the approach of Cordischi *et al.*,[19] a D value of 0.010 ± 0.001 cm^{-1} is obtained.

Apart from this species **II**, several other lines are observed in the spectrum, *e.g.* at 1100, 1900, 2800, and 4800 G, assigned to a species **III** (see below, Q-band data). Because they are spread over a broad field range, identification of these lines against the background may be difficult at low Mn concentrations, but by varying the Mn concentration, the relation between growing intensity of these lines and increasing Mn content was firmly established (Figure 4, a *vs* b). As the apparent splittings in this spectrum are of the same order as the X-band Zeeman energy, it was impossible to obtain the ZFS parameters from the X-band data alone.

(b) Q-band Spectra. The Q-band spectra of the same zeolite allowed us to assign these supplementary spectral lines to a species **III**. The zero-field splitting of this species **III** is dominated by a very large D value of 0.14 ± 0.01 cm^{-1} (Figure 5b). The groups of fine structure lines have been labeled on the spectrum by means of a calculated stick spectrum. With such a severe distortion of the Mn coordination, even small

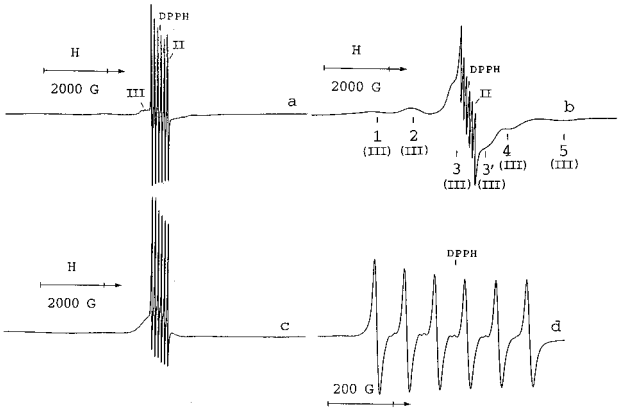

Figure 5. Q-band ESR spectra of hydrated MnNaA zeolites: (a and d) 0.1 wt %, 298 K, (b) 1.7 wt %, 298 K, (c) 0.1 wt %, 100 K. Note in a the superimposed sextets of species **II** and species **III**, about 350 G upfield. The positions in the stick diagram for species **III** in b were calculated with $D = 0.14$ cm^{-1}. Labels on the stick diagram as in Figure 3. Note the forbidden $\Delta M_S = \pm 1$, $\Delta M_I = \pm 1$ lines for species **II** in d.

deviations from the average D value become significant in comparison with the hyperfine constant A. As a result, hardly any hyperfine structure can be observed for **III**. Only at 298 K and low Mn concentration, the $M_S = +^1/_2 \leftrightarrow -^1/_2$, $\theta = 90°$ sextets of **II** and **III** are observed simultaneously (Figure 5a). The sextet of **III**, with $A = 0.0088 \pm 0.0002$ cm^{-1}, is centered 350 G downfield from that of **II**. With $D_{\mathbf{II}}$ smaller than 0.01 cm^{-1}, $D_{\mathbf{III}}$ is estimated to amount to 0.139 cm^{-1}, confirming the value from the stick spectrum in Figure 5b. Within the resolution of our data, there is no evidence for E being different from 0. Hence **III** is described as a strongly axially distorted Mn^{2+} complex.

As with species **I** in MnKA, cooling of MnNaA resulted in a resolution loss for species **III**. With MnNaA (0.1%) at 100 K, even the hyperfine structure of the central sextet of species **III** is lost (Figure 5c).

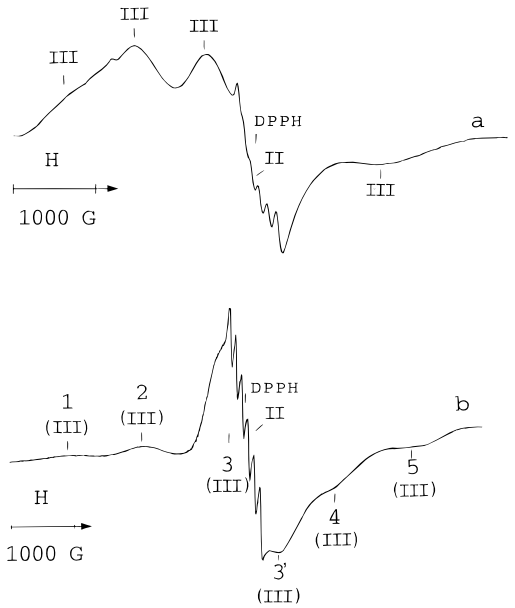

Figure 6. ESR spectra of 0.1 wt % hydrated MnLiA zeolite at 298 K, showing lines of species **II** and **III**: (a) X-band (9.44 GHz), (b) Q-band (35.0 GHz). Labels on b as in Figure 3.

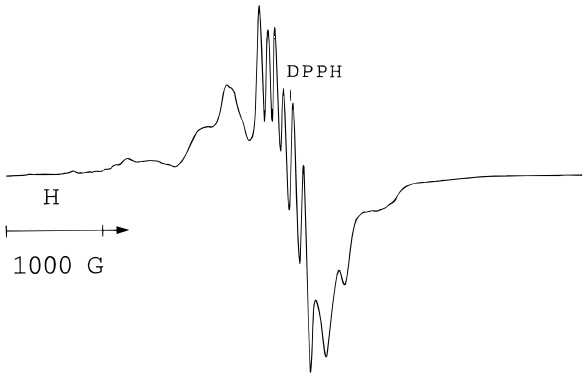

Figure 7. X-band ESR spectrum of hydrated MnCsNaA zeolite (0.1 wt % Mn) at 298 K.

The Q-band spectrum also yields a supplementary estimate for D in species **II**. At 298 K and low Mn concentration, the forbidden $\Delta M_S = \pm 1$, $\Delta M_I = \pm 1$ lines of species **II** are resolved (Figure 5d). Their amplitude varies between 1 and 2% of the amplitude of the allowed $\Delta M_S = \pm 1$, $\Delta M_I = 0$ lines. Following the approach of Poole *et al.*,[15] $D_{\mathbf{II}} = 0.009 \pm 0.002$ cm^{-1} is obtained, in reasonable agreement with the previous estimate from the X-band spectrum (Figure 4c).

3. Hydrated MnLiA Zeolites. In the spectra of Mn^{2+}-exchanged LiA, recorded at 298 or 100 K, the same species are detected as in the case of MnNaA. The sextet, centered at $g_{\text{eff}} = 2.006$, is ascribed to **II**, an almost octahedral Mn^{2+} species. All lines belonging to species **III** were also identified, in X- as well as in Q-band (Figure 6). However, the relative intensities of the signals of **II** and **III** are different in the Na^+ and the Li^+ zeolites. In NaA, the signal of species **II** is relatively much stronger than that in LiA, where species **III** dominates the spectrum. Quantification of these differences in terms of site population is however difficult in view of the very different field range spanned by **II** and **III**.

4. Hydrated MnCsKA, MnCsNaA, and $MnNH_4$A Zeolites. The overall aspect of the spectra of these samples is very close to that observed for MnKA (Figure 7). Only species **I**, with D between 0.035 and 0.039 cm^{-1}, is identified. The dependence of D on temperature is the same as in MnKA: D increases with decreasing temperature.

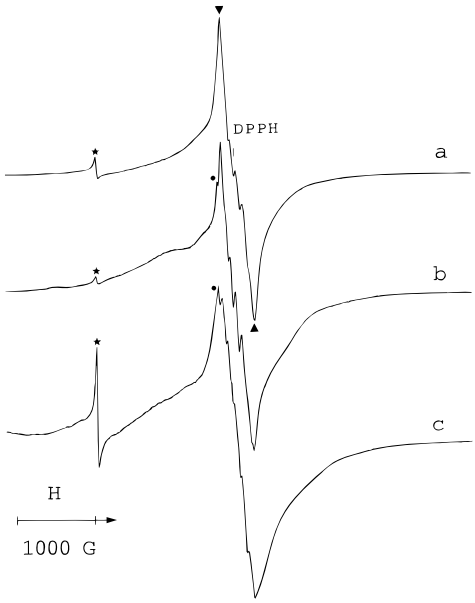

Figure 8. X-band spectra of fully dehydrated 0.025 wt % Mn A zeolites: (a) MnNaA, 298 K, (b) MnKA, 298 K, (c) MnNaA, 100 K. The peak-to-peak widths were calculated as indicated by triangles (▲). Dots (●) mark the supplementary line, downfield of the maximum, in MnKA (b) and cooled MnNaA (c). * = Fe impurities in the zeolite.

5. Dehydrated Zeolites. Dehydration at 673 K produces dramatic changes in the ESR spectra of MnNaA, MnKA, and MnLiA. In general, the spectra are less well defined than for the hydrated zeolites, and the presence of overlapping sextets close to $g = 2$, even at very low Mn content, indicates that the speciation is not always uniform.

(a) MnKA and MnNaA. The spectra of dehydrated MnKA and MnNaA are dominated by the central transition of the fine structure. At room temperature, the peak-to-peak width (calculated as labeled in Figure 8a) amounts to 400 ± 4 G, from which a maximum value $A = 0.0070$ cm^{-1} is obtained. In MnKA, an additional peak is observed downfield of the maximum in the first derivative spectrum (Figure 8b). This peak is also detected for MnNaA when the spectrum is recorded at 100 K (Figure 8c). The temperature-dependent spectral changes are fully reversible and indicate that the speciation fluctuates with temperature. The main, central transition is for both zeolites surrounded by wings, which are broader at lower temperatures. Such wings are typical for a distribution of the zero-field splitting parameters, and have been described for Mn^{2+} in glass environments,[14,20] or for frozen solutions of Mn^{2+} phosphate complexes.[17b] We label the overall appearance of Mn in these zeolites as species **IV**, characterized by (i) a small hyperfine constant, (ii) overlapping sextets near $g = 2$, and (iii) wings around the central absorption. It is stressed that species **IV** is a collective name for a distribution of similar Mn sites rather than a well-defined Mn complex.

(b) MnLiA. The X-band spectra of dehydrated MnLiA (Figure 9) display a line pattern which is recognized as that of an axially symmetric Mn ion, based on the analogy with the spectra in Figures 1a and 5b. The fine structure groups have been labeled on the spectra. From the positions of the noncentral fine lines, D is estimated at 0.032 ± 0.003 cm^{-1} at room temperature. There is no evidence for E being different from zero. There is a remarkable and reversible dependence of the spectrum on temperature (Figure 9b). At 100 K, D has increased by about 60%, to 0.050 ± 0.003 cm^{-1}. This species is denoted as species **V**. There seem to be small amounts of

(20) Griscom, D. L.; Griscom, R. E. *J. Chem. Phys.* **1967**, *47*, 2711.

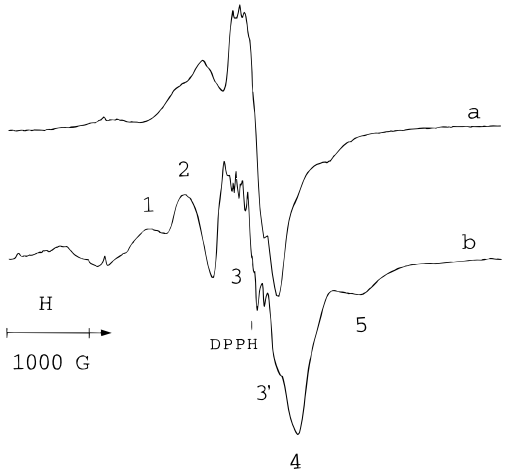

Figure 9. X-band spectra of fully dehydrated 0.025 wt % MnLiA zeolite, recorded at (a) 298 and (b) 100 K: 1 and 5, $M_S = \pm^5/_2 \leftrightarrow \pm^3/_2$, $\theta = 90°$; 2 and 4, $M_S = \pm^3/_2 \leftrightarrow \pm^1/_2$, $\theta = 90°$; 3, $M_S = +^1/_2 \leftrightarrow -^1/_2$, $\theta = 90°$; 3′, $M_S = +^1/_2 \leftrightarrow -^1/_2$, $\theta = 41.8°$.

other species, which prevent precise observation of the hyperfine structure around $g = 2$, and determination of A. In the low-field domain, a complex pattern with several Mn hyperfine sextets is observed. As for species **I**, these lines can be related to the forbidden $\Delta M_S = \pm 2$ transitions.

6. Rehydration of Zeolites. Even a very short exposure of the dehydrated zeolites to water causes a spectral change. After 5 min of rehydration, MnLiA, MnNaA, and MnKA display spectra as shown in Figure 10, parts a and b. A sextet with $A = 0.0081$ cm^{-1}, at $g_{\text{eff}} = 2.003$, is surrounded by wings. This species is labeled **VI**.

Further rehydration gradually and fully restores species **I** on MnKA. For MnNaA and MnLiA, species **III** is the first to reappear (Figure 10c). Only after extended water exposure is species **II** regenerated, but even then, the ratio **II**/**III** clearly remains lower in the rehydrated samples than before the dehydration.

Discussion

Table 1 gives an overview of the different Mn^{2+} species and their A and D parameters. Table 2 summarizes the dehydration−rehydration cycles for MnLiA, MnNaA, and MnKA.

Hydrated Zeolites. The overall spectroscopic picture allows us to divide the monovalent cations into two major groups. With K^+, Cs^+, and NH_4^+, species **I** is dominant. With Na^+ and Li^+, species **II** and **III** occur simultaneously, though in varying concentrations. The grouping of these cations basically corresponds to their size. The studies of Kevan on the spectroscopy of Cu^{2+} exchanged A zeolites have led to a very similar conclusion.[21−25] Our observations are therefore in excellent agreement with one of Kevan's major statements, namely that in A zeolites, exchanged with large monovalent cations, steric crowding makes it impossible to accommodate the regular, hexacoordinate hydrated transition metal ions. Thus steric arguments seem to prevail in the cation siting of both Cu and Mn A zeolites. This contrasts with the situation in X zeolites, where it was demonstrated both for Cu and for Mn that the cation location is determined by the competitive hydration of the metal ion and its co-cation.[2a,5]

It is well-established that in hydrated KA, CaNaA, and NH_4A zeolites, Cu^{2+} assumes an unusual pseudotetrahedral S_{II}* coordination, with the Cu^{2+} ion coordinated to three oxygen atoms of a 6-ring window of a sodalite cage, and with a water molecule as the fourth ligand.[22−24] In the case of Mn^{2+}, a tetrahedral coordination would be characterized by a decreased value of the hyperfine coupling constant A.[26] The A value of 0.0089 cm^{-1}, observed in KA, NH_4A, and the Cs zeolites, therefore rules out such a coordination. Nevertheless, the substantial deviation of the D value from 0 indicates that the

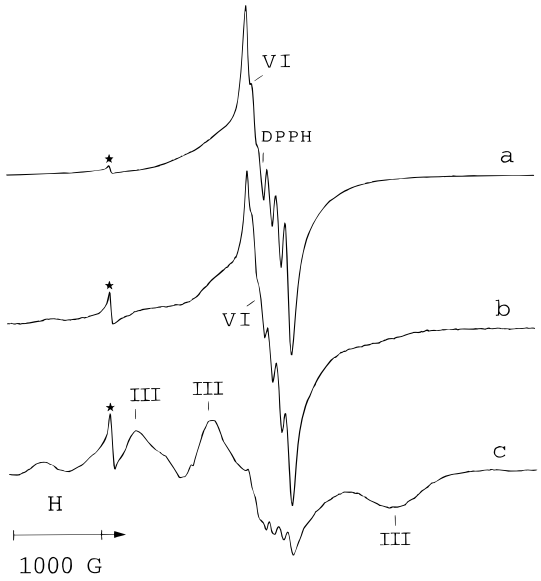

Figure 10. X-band spectra of partially rehydrated 0.025 wt % Mn A zeolites, recorded at 298 K: (a) MnLiA, after 5 min of water exposure, (b) MnNaA, after 5 min of water exposure, (c) MnNaA, after 30 min of water exposure. Initially, only species **VI** is visible. After 30 min, **III** dominates in MnNaA (compare Figure 10c with Figure 4a). * = Fe impurities in the zeolite.

Table 1. Spectroscopic Characteristics of Mn^{2+} Species in Zeolite A[a]

	$\lvert A\rvert$ (cm^{-1})	$\lvert D\rvert$ (cm^{-1})	proposed coordination	co-cation
I	0.0089	0.0356[b]	distorted octahedral	K^+, Cs^+, NH_4^+
II	0.0089	0.01	octahedral	Na^+, Li^+
III	0.0088	0.14	trigonal bipyramidal	Na^+, Li^+
IV	<0.0070	*c*	see text	Na^+, K^+
V	*c*	0.032[b]	trigonal	Li^+
VI	0.0081	*close to* 0	tetrahedral	Na^+, Li^+, K^+

[a] As expected, the g values of the Mn^{2+} species were all in the range 2.001−2.004. Significant deviations of g_{eff} from these values were always due to zero-field splitting. [b] Value at 298 K. [c] Value not determined.

Table 2. Evolution of Mn^{2+} Species in A Zeolites with Different Monovalent Co-cations during a Dehydration−Rehydration Cycle

co-cation	Li^+	Na^+	K^+
hydrated	**III (II)**	**II (III)**	**I**
↓	↓	↓	↓
dehydrated at 673 K	**V**	**IV**	**IV**
↓	↓	↓	↓
after 5 min of H_2O exposure	**VI**	**VI**	**VI**
↓	↓	↓	↓
after 30 min of H_2O exposure	**III**	**III (II)**	**I**

(21) Narayana, M.; Kevan, L. *J. Chem. Phys.* **1981**, *75*, 3269.
(22) Narayana, M.; Kevan, L. *J. Phys. C: Solid State Phys.* **1983**, *16*, 361.
(23) Anderson, M. W.; Kevan, L. *J. Phys. Chem.* **1987**, *91*, 1850.
(24) Narayana, M.; Kevan, L. *J. Chem. Soc., Faraday Trans. 1* **1986**, *82*, 213.
(25) Ichikawa, T.; Kevan, L. *J. Am. Chem. Soc.* **1981**, *103*, 5355.
(26) There is a correlation between the value of the hyperfine coupling constant A and the coordination number of Mn^{2+}: Abragam, A.; Bleaney, B. *Electron Paramagnetic Resonance of Transition Ions*; Clarendon Press, Oxford, 1970; p 440.

effect of the crowding on the Mn coordination sphere is strong, leading to an axially symmetric 6- or possibly 5-fold Mn coordination. A possible location for Mn^{2+} species **I** would be a pseudooctahedral S_{II}* position, in which Mn^{2+} would be coordinated to three lattice oxygens and to three water molecules, resulting in an imperfect antiprism, in which axial symmetry is maintained.

Hydrated NaA and LiA zeolites are much less sterically crowded, and it is not surprising that in these zeolites Mn^{2+} can assume a nearly octahedral coordination in species **II**. This species **II** may be a free $Mn(H_2O)_6^{2+}$ complex, as in NaX and NaY zeolites.[5] Species **III** is characterized by a substantially large value of D (0.14 cm^{-1}). At first sight it is difficult to understand why in NaA and LiA, with less steric crowding, the distortion of the Mn^{2+} coordination sphere is even more severe than in KA or NH_4A. However, for the case of MnNaA, X-ray diffraction data are available for evaluation of the Mn^{2+} siting. For a hydrated NaA zeolite, exchanged to a high degree with Mn^{2+}, Seff *et al*. found Mn^{2+} to be located mainly in site S_{II}, where it assumes a trigonal-bipyramidal coordination.[27] Three lattice oxygens of a 6-ring constitute the equatorial plane of the trigonal bipyramid, while two water molecules are located at its top and bottom, one inside the sodalite cage and one outside. Such a siting appears to match the coordination requirements derived from the parameters of species **III**. For an axially symmetric Mn trigonal bipyramid, a large D and a negligible E have indeed been reported.[28] The bond lengths reported by Seff ($Mn-O_{lattice} = 2.28$ Å; $Mn-O_{water} = 2.04$ Å) point toward a strong compression of the trigonal bipyramid, which is expected to result in a large D value, with E close to zero.

Dehydrated Zeolites. Species **IV** and **V** are both found in highly dehydrated A zeolites. While in faujasite structures dehydration often brings cations to a hexacoordinate position inside the hexagonal prisms, dehydrated A zeolites offer sites with a limited number of coordinating atoms to metal ions. An X-ray study by Seff *et al*. of Mn^{2+} in dehydrated NaA has suggested an S_{II} location for Mn^{2+}, where the metal ion is only coordinated by three lattice oxygen atoms of the zeolite six-ring.[27] This 3-fold coordination corresponds to a strong "axial elongation" of a trigonal bipyramid, by removal of the apical ligands. To our knowledge, the Mn ESR literature does not contain any species that is directly comparable to this situation, which makes it difficult to predict values for the ZFS parameters. However, in such a trigonal site, axial symmetry is preserved. This should lead to a large D, but to an E value close to zero.[28] The parameters of species **V** may well be compatible with such a coordination. Therefore it seems that in dehydrated MnLiA, Mn^{2+} resides in trigonal coordination at S_{II}. Our data are thus complementary to those of Klier,[29] who has previously described the unusual trigonal coordination of Ni^{2+} and Co^{2+} in dehydrated zeolite A by reflectance electronic spectroscopy.

The situation is less obvious for species **IV**. The low A value and the dehydrated state of the zeolite exclude 6- or 5-fold coordination.[26] Both 3-fold and pseudotetrahedral coordination are possible, but the 4-fold coordination is less likely in view of the results of the rehydration experiment (*see* below). In contrast to **V**, **IV** is a species not having a well-defined axial or rhombic distortion. Based on ESR data alone, it is therefore difficult to ascribe **IV** to a clearly defined lattice site.

Rehydrated Zeolites. Species **VI** is immediately formed upon water exposure of the coordinatively unsaturated species **IV** and **V**. The A value of species **VI** (0.0081 cm^{-1}) is intermediate between those of species **I**, **II**, and **III** (0.0089 cm^{-1}) and species **IV** (<0.0070 cm^{-1}). Species **VI** is clearly highly symmetric, e.g., close to octahedral or close to tetrahedral. The intermediate value of the A parameter rather favors the latter possibility. The location of Mn in species **VI** may be for instance site S_{II}*, with coordination to three oxygen atoms of the sodalite 6-ring and to one water molecule.

The order of appearance of the signals in MnNaA and MnLiA (first **III**, then **II**) is interesting. It suggests that **III** contains fewer water molecules in its coordination sphere than **II**. This is in full agreement with the proposals made above.

Conclusions

The nature of the different Mn^{2+} species and their interconversion proposed in this work are summarized in Tables 1 and 2. Of the six species presented, only species **II** (in hydrated NaA), **IV** (in dehydrated NaA), and **VI** (in partially hydrated NaA) had been reported in a previous ESR study.[6] The three species with the larger ZFS parameters (**I**, **III**, and **V**) were hitherto unknown. It seems therefore essential for a correct identification of Mn species to record ESR spectra at different frequencies and Mn concentrations. A similar approach has been applied recently in a re-investigation of the ZFS in organic Mn^{2+} complexes.[30] Moreover, we have tried, wherever possible, to estimate the ZFS parameters from the spectra by at least two independent criteria.

Our results also demonstrate that zero-field splittings can be directly observed in the powder spectra of Mn zeolites, which contrasts with all previous studies. In some cases, the uniformity of the Mn sites has been demonstrated beyond doubt, *e.g*. for MnAPOs with low Mn content, where ESR has been combined with ESEM.[7] In other studies, the presence of Mn in different coordination geometries, indicated by the observation of "wings" in the spectrum, may however have been underestimated. The observation of Fe in iron sodalite, where the sites are well-defined, and iron faujasite, with much more disorder, has led to similar caveat.[4]

The new species we propose (especially **III** and **V**) are similar to those found in related X-ray studies. Axial symmetry—whether in a trigonal bipyramid or in a planar 3-fold coordination—is very typical for transition metal sites in A zeolites, and our observations demonstrate that the D values are remarkably large. The sensitivity of the ZFS parameters to even minute changes in coordination is beautifully illustrated in the fully reversible temperature dependence of the ZFS, as documented for **IV**, but especially for **I** and **V**.

It is obvious that Mn siting in A zeolites is strongly affected by the co-cation present. This confirms the earlier observations for Cu^{2+} zeolites.

(27) Yanagida, R. Y.; Vance, T. B.; Seff, K. *Inorg. Chem*. **1974**, *13*, 723.

(28) Axially symmetric, trigonal bipyramidal complexes of Mn^{2+} are rare. To our knowledge, mainly the complexes with the protonated 1,4-diazabicyclo[2.2.2]octane (HL^+) have been studied. The ESR parameters of complexes of the types $[Mn(HL^+)_2X_3]X$ (X = Cl, Br) have been determined: Birdy, R. B.; Brun, G.; Goodgame, D. M. L.; Goodgame, M. *J. Chem. Soc. Dalton Trans.* **1979**, 149. For these axially symmetric five-coordinate complexes, D varies between 0.31 and 0.6 cm^{-1}; $E/D \leq 0.03$. The values of D for these complexes are considerably larger than what is observed for species **V**. However, it should be remembered that in the complexes of Goodgame et al., the trigonal bipyramid is subjected to an axial compression instead of an axial elongation. Moreover, the amine ligands in Goodgame's complexes are much stronger σ donors than the oxygen atoms of a zeolite lattice. Therefore, a quantitative comparison of the ZFS parameters is not straightforward.

(29) (a) Klier, K.; Ralek, J. *J. Phys. Chem. Solids* **1968**, *29*, 951. (b) Klier, K. *Adv. Chem. Ser*. **1971**, *101*, 480.

(30) Bryan Lynch, W.; Samuel Boorse, R.; Freed, J. H. *J. Am. Chem. Soc*. **1993**, *115*, 10909.

Although this work defines major features of the Mn siting in zeolite A as observed with ESR, some details of the coordination would benefit from additional structural insight, for example regarding the number of water molecules around Mn, or the interaction with various adsorbates. In this respect X-ray diffraction or particularly electron spin echo envelope modulation (ESEEM) studies may be helpful.

Acknowledgment. This work was sponsored by the U.S. Department of Energy. We thank Professor M. W. McElfresh and Shi-Li (Purdue University) for performing SQUID experiments. We are mostly indebted to Professor R. Linn Belford and Dr. A. Smirnov (ESR Research Center, University of Illinois at Urbana−Champaign) for the use of their Q-band spectrometer. We thank Professor F. Mabbs and Dr. D. Collison (University of Manchester, U.K.) for recording the Q-spectrum in Figure 3a. B.M.W. thanks the Belgian National Fund for Scientific Research (N.F.W.O.) for a position as research assistant, and D.D.V. is a postdoctoral researcher of N.F.W.O.

JA960012D